A new three dimensional biomimetic hydrogel to deliver factors secreted by human mesenchymal stem cells in spinal cord injury

Ilaria Caron [a,1], Filippo Rossi [b,1], Simonetta Papa [a], Rossella Aloe [a], Marika Sculco [a], Emanuele Mauri [b], Alessandro Sacchetti [b], Eugenio Erba [c], Nicolò Panini [c], Valentina Parazzi [d], Mario Barilani [d], Gianluigi Forloni [a], Giuseppe Perale [e], Lorenza Lazzari [d], Pietro Veglianese [a,*]

[a] *Dipartimento di Neuroscienze, IRCCS Istituto di Ricerche Farmacologiche "Mario Negri", via La Masa 19, 20156 Milan, Italy*
[b] *Dipartimento di Chimica, Materiali e Ingegneria Chimica "Giulio Natta", Politecnico di Milano, via Mancinelli 7, 20131 Milan, Italy*
[c] *Dipartimento di Oncologia, IRCCS Istituto di Ricerche Farmacologiche "Mario Negri", via La Masa 19, 20156 Milan, Italy*
[d] *Unit of Cell Therapy and Cryobiology, Fondazione IRCCS Ca' Granda Ospedale Maggiore Policlinico, via Francesco Sforza 35, 20122 Milan, Italy*
[e] *Department of Innovative Technologies, University of Applied Sciences and Arts of Southern Switzerland, SUPSI, via Cantonale, CH-6928 Manno, Switzerland*

A B S T R A C T

Stem cell therapy with human mesenchymal stem cells (hMSCs) represents a promising strategy in spinal cord injury (SCI). However, both systemic and parenchymal hMSCs administrations show significant drawbacks as a limited number and viability of stem cells in situ. Biomaterials able to encapsulate and sustain hMSCs represent a viable approach to overcome these limitations potentially improving the stem cell therapy. In this study, we evaluate a new agarose/carbomer based hydrogel which combines different strategies to optimize hMSCs viability, density and delivery of paracrine factors. Specifically, we evaluate a new loading procedure on a lyophilized scaffold (soaked up effect) that reduces mechanical stress in encapsulating hMSCs into the hydrogel. In addition, we combine arginine–glycine–aspartic acid (RGD) tripeptide and 3D extracellular matrix deposition to increase the capacity to attach and maintain healthy hMSCs within the hydrogel over time. Furthermore, the fluidic diffusion from the hydrogel toward the injury site is improved by using a cling film that oriented efficaciously the delivery of paracrine factors *in vivo*. Finally, we demonstrate that an improved combination as here proposed of hMSCs and biomimetic hydrogel is able to immunomodulate significantly the pro-inflammatory environment in a SCI mouse model, increasing M2 macrophagic population and promoting a pro-regenerative environment in situ.

1. Introduction

Many treatments (neuroprotective and/or neuroregenerative) have been proposed to counteract the neuropathological evolution of spinal cord injury (SCI) [1–5]. Among these, stem cell therapy represents a promising strategy [6–8] and accumulating data show that human mesenchymal stem cells (hMSCs) could be a real therapeutic approach in tissue repair after SCI [9–11]. Indeed, coherently with a multi-faceted SCI neuropathology, hMSCs are potentially able to counteract many harmful events and to sustain regeneration through several processes [10]. Different therapeutic effects have been proposed for hMSCs, but it is now well known that a paracrine effect [12], instead of a potential differentiation or transdifferentiation into neuronal or glial cells [13,14], is the most promising approach to exploit the therapeutic efficacy of the hMSCs [12,15,16]. In fact, hMSCs can act therapeutically by releasing exogenous trophic factors [17,18] and/or by modulating, through several factors, the immune system response [19–21]. However, different limitations are still to be overcome in using hMSCs as therapeutic opportunity in SCI. Specifically, cell therapy delivered systemically (intravenous injections) could lead to a limited efficacy due to the unfeasibility of the cells to cross the blood brain barrier

(BBB) and reach the injured site where they could be more useful [22–24]. Furthermore, a cellular systemic administration may give rise to potential side effects (pulmonary embolus) [25] that should not be underestimated. On the other side, an intrathecal injection could cause the loss of many cells in the intrathecal space or in the cerebrospinal fluid [24,26] or could stress and damage cells through mechanical forces [27], thwarting the effort to treat directly the injured site. Another proposed approach is a direct injection in the parenchyma, however, this could lead to a limited viability of stem cells due to both ischemia [28,29] and adverse environment in the injured site that follow SCI [29,30]. In order to overcome these drawbacks, new delivery strategies have been proposed by using original biomaterials [30–32]. Particularly, hydrogels offer the possibility to load and sustain both *in vitro* and *in vivo* hMSCs creating an optimal niche close to the injured site, but preserving them from the hostile tissue [30,33]. A variety of hydrogels (natural or synthetic) has been proposed as scaffolds able to allocate different stem cells [32,34–36]. Nevertheless, these scaffolds have been evaluated only for their own capacity to maintain the cell viability for a short time *in vitro* [37,38] and very few attempts have been proposed for an *in vivo* treatment [39,40]. However, an optimized scaffold able to act as a reservoir of neuroprotective factors secreted by hMSCs has not been developed and investigated yet. There are some concerns in using these scaffolds as potential reservoir *in vivo*. One relevant limit in the maintenance of stem cells allocated in a scaffold is the loss of adhesion due to the scaffold structural properties that do not represent appropriately a biological niche. In particular, a specific cell death (anoikis) occurred when hMSCs are not able to adhere to a biologic supportive niche such as an appropriate extracellular matrix (ECM) [6,41]. ECM has been demonstrated to be a crucial element to sustain hMSCs adhesion, trophic support and survival [42–44], maintaining and preserving also their stemness [45]. So far, only a few studies have been performed to mimic a sustainable ECM for hMSCs in 3D scaffolds. But just one single molecule at time (e.g. fibrin, laminin, collagen, fibronectin or arginine–glycine–aspartic acid (RGD) peptide) has been proposed and characterized [35,46–48]. However, these approaches could not be able to favor appropriately hMSCs adhesion to the scaffold since they do not mimic native ECM that is a combination of several proteins, cytokines and growth factors [49]. Thus, an alternative supporting strategy able to improve the adhesion and viability of the stem cells into the hydrogel is needed. In this study, we propose a new biomaterial coated with 3D ECM, with the aim to create a more optimized niche able to better sustain hMSCs viability and healthy.

2. Materials and methods

2.1. Hydrogels synthesis

Hydrogels were prepared by batch reaction in a phosphate buffered saline solution (PBS, Sigma–Aldrich) at about 80 °C in which a polymeric solution was achieved by stirring polymers: carbomer 974p (branched polyacrylic acid, MW = 1 MDa, Fagron), agarose (MW = 300 kDa, Invitrogen) and polyethylene glycol (PEG, MW = 2000 Da, Sigma–Aldrich). The composition is: 9 mL PBS, 50 mg carbomer 974p, 300 mg PEG and 50 mg agarose [50]. The reaction pH was indeed kept neutral with NaOH 1 N. The effective gelation and reticulation were achieved by means of electromagnetic stimulation (500 W power irradiated) for 15 s per 5 mL of polymeric solution. The mixing reactor was kept closed to avoid any eventual loss of solvent vapors, and the gelation was then achieved in a 48 multiwell cell culture plate (0.25 mL each with the cylinder diameter of 1.1 cm) in which the gelling solution was poured during cooling.

2.2. RGD hydrogel synthesis

RGD functionalized hydrogels (HG RGD) were prepared as presented in previous work [51]. Briefly, the peptide was synthesized manually using the stepwise solid phase Fmoc method and then functionalized with azide group (RGD-azide). Polyacrylic acid (PAA, MW = 130 kDa) with propargyl group was synthesized and dialyzed (PAA-propargyl). RGD-azide (25 mg) was suspended in THF (5 mL) and PAA-propargyl (78 mg) was dissolved in distilled water (10 mL). Two solutions were blended together and added copper iodide (2.2 mg, 0.0116 mmol) and sodium ascorbate (2.2 mg, 0.0111 mmol). The reaction mixture was allowed to stir for 24 h at 60 °C. Subsequently, it was cooled at 25 °C and dialyzed against acid solution consisting of distilled water (2000 mL), sodium chloride (11.2 g) and HCl 37% w/w to reach pH = 5; dialysis occurred for three days, with daily replacement of dialysis solution. Finally, the mixture was frozen at −20 °C and then lyophilized and stored for further use. PAA functionalized is blended in PBS at room temperature, until complete dissolution together with branched PAA (carbomer 974p). PEG is subsequently added and the system kept stirred for 45 min; then the mixing is left to settle. The composition is: 9 mL PBS, 40 mg carbomer 974p, 10 mg PAA-RGD, 300 mg PEG, 50 mg agarose. NaOH 1 N is then added to adjust pH to 7.4 and then, after the addition of agarose powder which is not soluble at room temperature, the system is subjected to electromagnetic stimulation (500 W irradiated power), heating up to 70–80 °C to induce condensation reactions, through interconnections of hydroxyl groups. PAA carboxyl groups constitute crosslinking sites to be reacted with hydroxyl groups from agarose and PEG, forming ester bonds and altogether giving rise to the three dimensional matrix. Mixing reactor was kept closed to avoid any eventual loss of solvent vapors and the gelation was then achieved in a 48 multiwell cell culture plate (0.25 mL each and with the cylinder diameter of 1.1 cm) where the gelling solution was poured during cooling. In order to obtain lyophilized scaffolds, hydrogels were frozen on dry ice for 5 min, transferred at −80 °C over night and then dried in the following conditions: 1 mbar and −45 °C. The lyophilized gels were sterilized for at least 3 h by UV illumination before cells seeding. Obtained freeze-dried hydrogels resemble a sponge and for this reason here after they are indicated as sponge-like hydrogels.

2.3. Cord blood human mesenchymal stem cells culture

Umbilical cord blood was collected from normal deliveries, after written informed consent, in a multiple system bag (Macho-pharma) containing 29 mL of citrate phosphate dextrose as anticoagulant. Briefly, whole blood was centrifuged at 1900 rpm for 15 min, the plasma subsequently discarded and the buffy coat with a portion of red blood cells collected was immunodepleted of CD3+, CD14+, CD38+, CD19+, glycophorin A and CD66b+ using a commercial kit RosetteSep® (StemCell Technologies), according to manufacturer's instructions. In summary, the sample was incubated with 50 μL/mL RosetteSep MSC enrichment cocktail for 20 min at room temperature to isolate MSC precursors.

The buffy coat was then diluted 1:2 with phosphate buffered saline (PBS; Gibco), ethylenediaminetetraacetic acid (EDTA; Sigma–Aldrich) and human serum albumin (HAS; Kedrion), and separated under standard density gradient conditions (Ficoll Paque Plus 1.077 ± 0.001 g/L; GE Healthcare). After, mononuclear cells were then plated at 1×10^6 cells/cm^2 in standard medium: alphaMEM-GlutaMAX (Invitrogen) supplemented with 20% fetal bovine serum (FBS, Life Technologies).

Cultures were maintained at 37 °C in a humidified atmosphere containing 5% CO_2. After 48 h, non-adherent cells were removed and fresh medium was added. At 80% confluence, the cells were

harvested using 25% TrypLE Select 1× (Gibco) and subcultured at a concentration of 4×10^3 cells/cm^2 until passage 3 [52]. From passage 3, when the cell population was homogenous with no hematopoietic contamination, human mesenchymal stem cells (hMSCs) were used for *in vitro* and *in vivo* experiments. hMSCs populations derived from ten umbilical cord blood unit, already established and fully characterized for optimal growth properties and defined as long living (LL)-CBMSCs [52], were used for this study. hMSCs identity definition is presented as supplementary information (Fig. S1). All experiments have been conducted according to the principles expressed in the declaration of Helsinki.

2.4. Classic loading

hMSCs were harvested and suspended at a density of 5×10^6 cells/mL in growth medium supplemented with 2× FBS. Hydrogels were prepared as described above by mixing polymer powders in PBS. The hydrogel was heated at 80 °C to start gelation. When hydrogel solution temperature fell below 40 °C, a 1:1 solution of cells and hydrogel was prepared (20 μL cells and 20 μL hydrogel). Cells and hydrogel were mixed together and the final solution was pipetted into polystyrene cylinders (5 mm diameter) and let it polymerize for 30 min in incubator at 37 °C. After polymerization, growth medium was added to polymerized hydrogels containing cells. Each hydrogel contained approximately 100,000 cells.

2.5. Sponge-like loading

hMSCs were harvested and suspended at a density of 1.25×10^6 cells/mL in growth medium. 80 μL of cells were added directly onto the sponge-like hydrogel (40 μL for each side). Hydrogels were let to swell for 30 min in incubator at 37 °C and then 1 mL of growth medium was added. Each hydrogel contained approximately 100,000 cells.

2.6. ECM quantification

After 1, 7, 14 and 21 days after hMSCs seeding on sponge-like HG RGD, the ECM deposition was quantified by Sirius Red staining. Sirius Red is a method for collagen staining and it allows the evaluation of the ECM deposition overtime [53,54]. In particular, hydrogels were decellularized with an ammonium hydroxide buffer containing Triton X-100, in order to remove cells but preserving ECM deposition, as reported by Prewitz et al. [55] Briefly, hydrogels were immersed in a warm solution containing 0.5% of Triton X-100 and 20 mM of ammonium hydroxide in PBS in fast agitation for 10 min. After 3 washes in PBS, the ECM was stained by picro Sirius Red solution composed of 1% of Sirius Red (Direct Red 80, Sigma–Aldrich) in a saturated aqueous solution of picric acid (Sigma–Aldrich) that was added to the hydrogels and maintained for 30 min at room temperature. Then the excess of staining was eliminated by 3 washes with acidified water (0.5% of acetic acid in distilled water). To quantify the ECM staining, the Sirius Red dye was extracted from the hydrogel through a solution of 0.05 M NaOH and methanol [1:1], in which hydrogels were immersed for 1 h. The obtained solution was evaluated by a spectrophotometer (Infinite M200, TECAN) at an absorbance of 540 nm.

2.7. Extracellular matrix (ECM) deposition

hMSCs were let to grow for 14 days on sponge-like HG RGD. Then all the liquids around hydrogel were removed and the hydrogels were frozen on dry ice for 5 min and then transferred at −80 °C overnight. The lyophilization procedure was conducted as reported above.

2.8. Cellular density and viability analyses in vitro

hMSC density and survival were determined by analyzing confocal images of live cells stained with calcein AM (1:1000, Invitrogen). Calcein AM is a non-fluorescent cell-permeant dye that is converted to a green-fluorescent calcein after acetoxymethyl ester hydrolysis by intracellular esterases. It was added to the well containing hydrogels for 30 min at 37 °C. Then the medium was removed and substituted with fresh growth medium. hMSCs within the scaffold were stained with Calcein AM and acquired by confocal microscope (Olympus Fv1000) equipped with Laser 488. Three optical sections of the hydrogels spaced of 80 μm were acquired at 10× magnification. The number of calcein AM positive cells was measured using a “surface detection” tool of Imaris software (Bitplane). The number of cells was evaluated as cellular density (cells/mm^2).

2.9. Scanning Electron Microscopy (SEM)

SEM analysis was performed in sponge-like HG RGD and HG RGD + ECM after 1 day from hMSCs seeding. Each hydrogel was fixed overnight in a buffer containing 1.5% of glutaraldehyde in 0.1 M of sodium cacodylate. Then hydrogels were dehydrated in an increasing scale of alcohols and frozen at −80 °C overnight. Before SEM analysis hydrogels were dried and gold coated and then analyzed at 10 kV with Evo 50 EP Instrumentation (Zeiss).

2.10. Cellular differentiation assays

hMSC differentiation after encapsulation in HG RGD + ECM was assessed by Real Time PCR. The gene expression for the three main mesodermal lineage differentiation (osteogenic, chondrogenic and adipogenic) was performed. Sponge-like HG RGD + ECM containing hMSCs cultured for 21 days in growth medium were analyzed. As positive control, hMSCs cultured in HG RGD for 21 days and treated with differentiation media were analyzed. In particular, to promote adipogenesis, osteogenesis and chondrogenesis, commercial media (Lonza S.p.A.) were used, and the manufacturer's protocols were followed or slightly modified [52]. For information about differentiation media full composition please refer to www.lonza.com. Data are expressed as fold change compared to steady-state undifferentiated hMSCs (negative control). Hydrogels were homogenized and RNA was extracted using RNeasy mini kit (Qiagen), according to manufacturer's instructions. Briefly, hydrogels containing cells were suspended in QIAzol Lysis Reagent and homogenized with a tissue grinder. Chloroform was added to the homogenate and a phase extraction performed. 0.3 mL of the aqueous phase were added to 450 μL of ethanol and loaded onto an RNeasy column. The column was washed and RNA eluted in 50 μL of RNAse free water. RNA was quantified by a spectrophotometer (Infinite M200, TECAN) at 260 nm for all samples, frozen at −20 °C and stored until use.

Reverse transcription was carried out using iScriptTM cDNA Synthesis Kit (Bio-Rad Laboratories Ltd). Real time PCR was performed on a CFX96 Real Time System using Sso FastEva Green Super mix (Bio-Rad), according to the manufacturer's instructions. The expression of the following genes was evaluated: alkaline phosphatase (ALP), runt-related transcription factor 2 (RUNX2) and osterix are genes involved in various stages of osteogenic differentiation [56]; aggrecan (ACAN) and type 10 collagen alpha 1 (COLLX) are genes correlated to the late phase of chondrogenic differentiation [57]; adipsin and fatty acid binding-protein 4 (FABP4) are genes actively expressed during the late phase of adipogenic differentiation [58]. Ribosomal protein large P0 (RPLP0) gene expression was used as control [59]. Specific primers used are listed below:

- adipsin (Fw: GACACCATCGACCACGA; Rev: CACGTCGCAGAGA GTTC);
- FABP4 (Fw: AAAGAGAAAACGAGAGGATGA; Rev: AACGTCCCTTG GCTTATG);
- RUNX2 (Fw: AAGGCTGCAAGCAGTATTTACAA; Rev: CTCGGATCCC AAAAGAAGTTTTGCT);
- osterix (Fw: CCTGCTTGAGGAGGAAGTTCA; Rev: AGAGTTGTTGA GTCCCGCAG);
- ALP (Fw: TACAAGGTGGTGGGCGGTGAACGA; Rev: TGGCGCAGGG GCACAGCAGAC);
- ACAN (Fw: TCGCCAGGTGTGTGGGACTGA; Rev: ACTCAGCGAGT TGTCATGGTCTGA);
- COLLX (Fw: ACTCCCAGCACGCAGAATCCA; Rev: TGGGCCTTTTAT GCCTGTGGGC);
- RPLP0 (Fw: TGTGGGCTCCAAGCAGATGCA; Rev: GCAGCAGTTTC TCCAGAGCTGGG).

2.11. Surgery

Procedures involving animals and their care were conducted in accordance with institutional guidelines at the IRCCS — Institute for Pharmacological Research "Mario Negri" in compliance with national (Decreto Legge nr.116/92, Gazzetta Ufficiale, supplement 40, February 18, 1992; Circolare nr. 8, Gazzetta Ufficiale, July 14, 1994) and international laws and policies (EEC Council Directive 86/609, OJL 358, 1, Dec. 12, 1987; Guide for the Care and Use of Laboratory Animals, US National Research Council, 8th edition, 2011).

Adult C57BL/6J female mice (23–30 g) were anesthetized by intraperitoneal injection of ketamine hydrochloride (IMALGENE, 100 mg/kg) and medetomidine hydrochloride (DOMITOR, 1 mg/kg). Before surgery, animals received an antibiotic and analgesic subcutaneous treatment with Ampicillin (50 mg/kg) and Buprenorfin (0.15 mg/kg), respectively. The back of the animals was shaved at the dorsal level and a cutaneous incision was made to expose the backbone. Animals were placed on a Cunningam Spinal Cord Adaptor (Stoelting) mounted on a stereotaxic frame. A laminectomy at the T12 level was done to uncover the lumbar spinal cord. A moderate compression of the spinal cord was obtained using an aneurysm clip (30 g compressive force for 60 s) as described previously [50].

2.12. Cellular staining for in vivo tracking

Before the seeding in the scaffold, hMSCs were stained with the marker of cellular viability 5-6-Carboxyfluorescein diacetate N-succinimidyl ester (CFDA-SE, Sigma–Aldrich), a cell-permeant fluorescent based tracer for long-term viable cell labeling. In particular, suspended cells were incubated for 30 min at 37 °C with pre-warmed CFDA-SE solution in PBS (final concentration 5 μM). Then, 5 times the original staining volume of medium was added in order to remove any free dye remaining in the solution. Cells were then incubated for 5 min at 37 °C. Finally, cells were centrifuged at 300 g for 10 min, resuspended in pre-warmed complete culture medium and deposited in sponge-like HG RGD + ECM.

2.13. In vivo positioning of hMSC in HG RGD + ECM

hMSCs were encapsulated for 1 day in sponge-like HG RGD + ECM. Then, hMSCs loaded HG RGD + ECM (a total of 25,000 cells/animal) was positioned in correspondence to the injury level. The hMSC loaded hydrogel was secured by applying a cling film on the top, sealed at the edges with a tissue adhesive (3M Vetbond). Dorsal muscles were then juxtaposed using absorbable sutures and the skin was sutured. After the surgery, the animals were kept on a warm pad for 30 min and then placed in separated cages with facilitated access to food and water for recovery.

As controls for subsequent analyses, other groups of animals were taken into consideration: animals treated with hMSCs directly injected in the parenchyma, animals treated with conditioned medium (CM) directly injected in the parenchyma, animals treated with HG RGD + ECM loaded only with CM. hMSCs and CM were injected as follows: hMSCs were suspended at a concentration of 50,000 cells/μL and, using a 30G needle associated to the stereotaxic, they were injected (0.5 μL/site) very close to the epicenter of the lesion (rostral edge) with a flow rate of 0.25 μL/min. The needle was positioned at the midline, then it was deepened into the parenchyma to 0.6 mm below the pia mater. For the other groups, CM was obtained after 1 day culture of hMSCs in culture plates. Using the same protocol adopted for hMSCs seeding, CM was loaded into the HG RGD + ECM. Briefly, 80 μL of CM were added directly onto the sponge-like hydrogel (40 μL for each side). Then, hydrogels were let to swell for 30 min in incubator at 37 °C.

2.14. hMSCs in vivo tracking

In vivo tracking of viable hMSCs stained with CFDA-SE was obtained using a stereomicroscope (Olympus SZX10). Animals with the backbone and the hydrogel exposed were evaluated by a stereomicroscope and a series of images of the entire hydrogel were acquired at 1.6×. Hydrogels acquisitions were made the same day of the positioning (day 0) and at 3 or 9 days after the positioning. CFDA-SE positive cells were counted using the "spots detection" tool of Imaris software (Bitplane). The number of stem cells detected in each hydrogel at day 0 was considered as 100% of survival. The number of cells detected in the same hydrogels at 3 or 9 days was then reported as a percentage of survival in respect to the same hydrogel at day 0.

2.15. In vivo positioning of Hoechst hydrogels

After the spinal cord compression, sponge-like HG RGD was loaded with 20 μL of 0.7 mg/mL Hoechst 33258 pentahydrate (bisbenzimide) (Life technologies) and positioned at the injury level. The animals were then divided in 2 groups, one with only the positioning of Hoechst-loaded hydrogels onto the injury site, the other where Hoechst-loaded hydrogel was secured by applying a cling film on the top, sealed at the edges with a tissue adhesive (3M Vetbond). Dorsal muscles were then juxtaposed and the skin was sutured. After the surgery, the animals were kept on a warm pad for 30 min and then placed in separated cages with facilitated access to food and water for recovery.

2.16. Spinal cord transcardiac perfusion

For histological evaluations, after 9 days from the Hoechst hydrogels positioning, mice were deeply anesthetized with ketamine hydrochloride (IMALGENE, 100 mg/kg) and medetomidine hydrochloride (DOMITOR, 1 mg/kg) and transcardially perfused with 40 mL of sodium phosphate buffered (PBS) 0.1 M, pH 7.4, followed by 50 mL of 4% paraformaldehyde solution in PBS. Spinal cords were then removed, postfixed overnight in the same fixative and then transferred to 30% sucrose in PBS at 4 °C overnight for cryopreservation and stored at 4 °C until use. The spinal cord was embedded in OCT compound, frozen by immersion in N pentane at 45 °C for 3 min and then stored at 80 °C. Frozen tissues were sectioned at 50 μm on a cryostat at −20 °C. Starting from the rostral edge (about 6 mm rostral to the epicenter), one section every 10 was mounted on slides for a total of 24 sections (about 12 mm sectioned) and coverslipped with a 50% glycerol solution in PBS before to proceed with acquisition at 10× magnification by confocal

microscopy (Olympus Fv1000, Laser 405).

2.17. Hoechst distribution analysis

The quantification of the Hoechst distribution and penetration into tissue was performed using the free software ImageJ, making a threshold based on signal intensity. The thresholded area was then quantified and showed as total Hoechst delivery area evaluated in the tissue. Furthermore, an evaluation of the Hoechst signal in each slice sampled (each 10 sections) in a spinal cord region of 12 mm was performed. Four animals per group were analyzed.

2.18. Flow cytometry

After 9 days of treatment by hMSCs loaded HD RGD + ECM, animals were decapitated and spinal cords were rapidly flushed out by the column. The region around the epicenter of the lesion was put on a cell strainer (40 μm nylon mesh) and a cell suspension was obtained by pressing with the plunger of a 10 mL syringe. Then the cell strainer was washed with 5 mL of GKN solution pH 7.4 (8.00 g/L NaCl, 0.40 g/L KCl, 0.93 g/L NaH_2PO_4, 1.42 g/L Na_2HPO_4, 2.00 g/L D-glucose, 0.02% BSA). For each sample, 1.5 mL of the cell suspension obtained was centrifuged at 2000 rpm for 5 min and pellet cells were resuspended in 500 μL of FACS blocking (1% BSA, 5% FBS in PBS). After 20 min of incubation in FACS blocking at 4 °C, primary antibodies CD11b-APC780 (ebioscience [1:100]) and CD45-PE (BDbioscience [1:100]) were added and incubated for 20 min at 4 °C in the dark. Then, 1 mL of PBS was added and samples were centrifuged at 2000 rpm for 5 min. Pellet cells were resuspended in 1 mL of FACS blocking before proceeding to FACS analysis. A specific isotype antibody staining was performed as negative control. Immunophenotyping analyses were performed on at least 1,500,000 cells for each sample by using MoFlo Astrios instruments (Beckman Coulter) equipped with 488, 546 and 640 nm lasers. Fluorescence pulses were detected using a band pass filter 671/20 for CD45, 795/70 for CD11b. Results were analyzed using Kaluza software (Beckman Coulter). Data are expressed as percentage of positive cells per gated event.

2.19. RNA analysis

After 9 days of treatment by hMSCs loaded HD RGD + ECM, animals were decapitated and spinal cords were rapidly flushed out by the column. The region around the epicenter of the lesion was rapidly frozen on dry ice and stored at −80 °C until use. Total RNA was obtained from tissues using RNeasy Mini Kit (Qiagen), as already reported above. Samples of total RNA were treated with DNAse (Applied Biosystems) and reverse-transcribed with random hexamer primers using Multi-Scribe Reverse Transcriptase (TaqMan Reverse transcription reagents; Applied Biosystems). Real-time RT-PCR was performed according to the manufacturer's instructions using 2 ng of cDNA, 200 nmol of each primer and SYBR Green master mix (Applied Biosystems) in a total volume of 20 μL. Levels of PCR product were measured using SYBR Green fluorescence collected during Real-Time RT-PCR on an Applied Biosystems 7300 system. The expression of the following genes was analyzed:

- YM1 (Fw: TCTGGTGAAGGAAATGCGTAAA; Rev: GCAGCCTTGGA ATGTCTTTCTC);
- Arginase I (Fw: CATGGGCAACCTGTGTCCTT; Rev: TCCTGGTACAT CTGGGAACTTTC);
- IL-1β (Fw: AGTTGACGGACCCCAAAAGA; Rev: GGACAGCCCAG GTCAAAGG);
- TNFα (Fw: AGACCCTCACACTCAGATCATCTTC; Rev: TTGCTACGAC GTGGGCTACA);
- β-Actin (Fw: CGCGAGCACAGCTTCTTT; Rev: GCAGCGATATCGT CATCCAT).

β-Actin was used as reference gene and relative gene expression levels were determined according to the manufacturer's ΔΔCt method (Applied Biosystems). Data are expressed as fold change from untreated injured mice spinal cord samples.

2.20. Statistical analyses

Statistical analyses were performed by Prism software (Graphpad). Statistical tests applied were Mann–Whitney test, one-way ANOVA or two-way ANOVA followed by Bonferroni's post hoc test, as reported in figure legends. Data are presented as mean ± SEM.

3. Results

3.1. Extracellular matrix improves hMSCs adhesion and survival in biomimetic hydrogels

In order to optimize and evaluate the hMSCs adhesion and viability several hydrogel compositions and different loading protocols were developed and tested. Specifically, we synthesized and functionalized the following scaffolds: carbomer/agarose/polyethylene glycol (PEG) based hydrogel incorporating RGD adhesive peptide (HG RGD) or HG RGD with a 3D ECM deposition (HG RGD + ECM) (Fig. 1 A). Furthermore, different loading protocols have been tested: hMSCs were mixed with the hydrogel during its polymerization (hereafter termed classic loading, Fig. 1 B a) or fluidically loaded into lyophilized HG, the latter acting like a sponge able to soak up cells together with the medium solution (hereafter termed sponge-like loading, Fig. 1 B b). Cell survival, adhesion and density within the scaffolds were evaluated by labeling live cells with Calcein AM over time and expressed as number of positive cells per mm^2. To evaluate the different loading protocols proposed we used a HD RGD scaffold demonstrating a significant increase of hMSCs survival at both 14 and 21 days after a sponge-like loading compared to the classic loading (Fig. S2 A, B). Moreover, a partial spindle shape morphology was detected only in the sponge-like HG RGD, but not in the classic loading HG RGD (Fig. S2 A, B), suggesting that a reduced stress and a better adhesion were obtained when hMSCs were loaded by fluidic diffusion into the hydrogel. In order to further increase cell density and adhesion in the scaffold, we developed a HG RGD containing a 3D deposition of ECM potentially able to provide more anchorage for hMSCs and a better supporting environment. We first seeded hMSCs into HG RGD and we measured the ECM deposited over time. A progressive ECM deposition was observed from 1 up to 14 days, where ECM deposition reaches a “plateau” (Fig. S3). Thus, for a second hMSCs seeding, we decided to deposit ECM up to 14 days and then we lyophilized the HG RGD + ECM to allow a new encapsulation of hMSCs by a sponge-like loading (see the Materials and methods section and Fig. 1 A and B). Noteworthy, analyzing hMSCs within HG RGD + ECM, we found a markedly increased cell adhesion to the biomimetic substrate. Indeed, already at the first day after seeding, HG RGD + ECM provided an anchorage for hMSCs. The almost totality of hMSCs showed a healthy spindle shape morphology 1 day after the encapsulation with a significantly higher long lasting cell density (3 fold higher) compared to HG RGD (Fig. 2 a).

3.2. SEM analysis shows a high hMSC density with a spindle shape morphology in HG RGD + ECM

In order to further characterize hMSC adhesion, morphology and density within both HG RGD and HG RGD + ECM, we

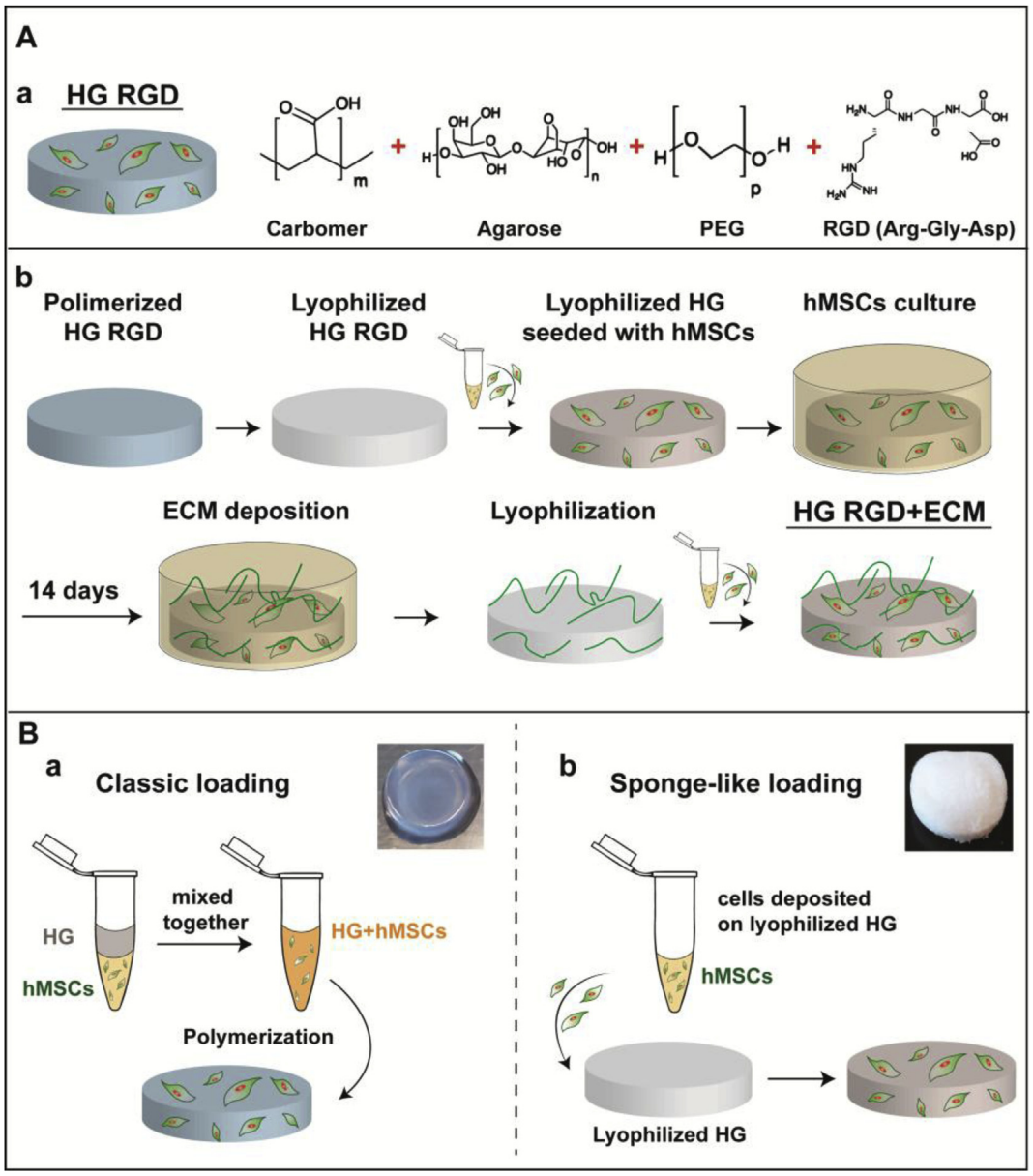

Fig. 1. Schematic representation of different hydrogel compositions and loading protocols tested. (A) Hydrogel compositions tested were: RGD (arginine–glycine–aspartic acid) adhesive peptide incorporated into HG (HG RGD, a) or HG RGD with a 3D-ECM deposition (HG RGD + ECM, b). The latter was obtained by different steps such as represented in panel b. (B) Cartoons represent the different loading protocols tested: a classic loading way in which hMSCs were mixed with HG RGD during its polymerization (a, inset) or sponge like loading in which hMSCs were loaded with a soaked up effect into lyophilized HG RGD (b, inset).

performed Scanning Electron Microscopy (SEM). SEM evaluation showed an irregular surface among the network mesh, varying from rough, in HG RGD, to smooth, in HG RGD + ECM, the latter revealing the ECM deposition (Fig. 3). Furthermore, we observed more clusterized and spindle shape hMSCs attached to the HG RGD + ECM biomimetic scaffold compared to HG RGD, confirming a healthy state and a higher cell adhesion within HG RGD + ECM (Fig. 3).

3.3. *HG RGD + ECM preserves hMSC stemness*

In order to demonstrate that HG-RGD + ECM did not spontaneously induce any typical MSC differentiation thus preserving the hMSC stemness for a long time, even when encapsulated, we compared the gene expression profile of hMSCs encapsulated in HG-RGD + ECM with the same hMSCs but differentiated towards osteocytes, chondrocytes and adipocytes (Fig. 4 D). Genes evaluated were alkaline phosphatase (ALP), Runt-related transcription factor 2 (RUNX2) and Osterix for osteocytes, Aggrecan (ACAN) and collagen type X (COLLX) for chondrocytes, whereas Adipsin and Fatty acid binding-protein 4 (FABP4) for adipocytes. The analysis was conducted on hMSCs encapsulated within HG RGD + ECM for 21 days and subsequently isolated for PCR analysis. As positive control we used hMSCs loaded within HG RGD and treated with differentiating media up to 21 days. We observed a significantly higher gene expression in positive controls compared to untreated hMSCs loaded in HG-RGD + ECM for all genes tested (Fig. 4 A, 4 B and 4 C) demonstrating that HG-RGD + ECM per se was not able to stimulate any classical mesodermal differentiation preserving stemness for a long time.

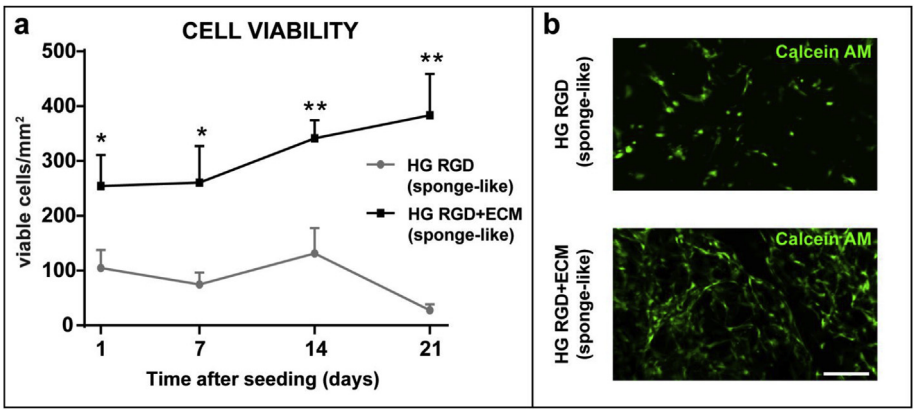

Fig. 2. HG RGD + ECM shows a high hMSC viability with a spindle-shape morphology *in vitro*. (a) Graph representing viability of hMSCs loaded in sponge-like HG RGD or sponge-like HG RGD + ECM scaffolds. Cell viability was evaluated over time by labeling live cells with Calcein AM. Already at the first day after seeding, HG RGD + ECM displays a significantly higher viability and density of hMSCs compared to HG RGD. This high cellular density is preserved over time. In the graph the cell density within the hydrogels is reported as number of calcein AM positive cells per mm^2. Statistical analysis: Mann Whitney test for each time point. Mean ± SEM is reported. (*) $p < 0.05$. (**) $p < 0.01$. $n = 8$ per group. (b) Representative images showing hMSCs stained with Calcein AM in sponge-like HG RGD and sponge-like HG RGD + ECM scaffolds. Already at the first day after seeding here represented, the almost totality of hMSCs within HG RGD + ECM shows a healthy spindle shape morphology. Differently, only a very few hMSCs in HG RGD show a partial adhesion to the scaffold and a spindle shape morphology. Scale bar represents 200 μm.

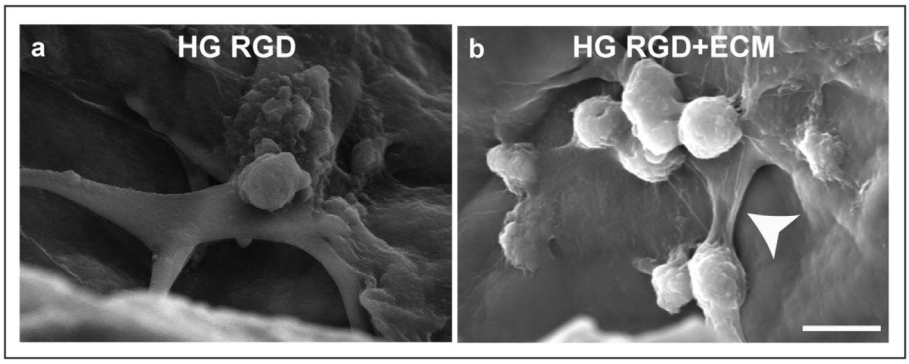

Fig. 3. Morphological analysis of HG scaffolds by SEM. Representative SEM images of both sponge-like HG RGD (a) and sponge-like HG RGD + ECM (b) scaffolds. The ECM deposition is represented by irregular surface among the networks mesh in HG RGD + ECM (arrowhead). A higher cellular density and a higher cell attachment to the substrate can be observed in HG RGD + ECM. Scale bar represents 10 μm. 3000×.

3.4. hMSCs loaded within HG RGD + ECM preserve viability up to 9 days in vivo

Since HG RGD + ECM showed an optimized viability, a higher cellular adhesion and a preserved stemness of hMSCs after a sponge-like loading *in vitro*, we decided to evaluate the behavior of hMCSs loaded in HG RGD + ECM also *in vivo*. To do that, after the implantation in the injured site, we performed a longitudinal study by means of intravital microscopy. Cell survival was evaluated over time by labeling live stem cells with CFDA-SE (a vital fluorescent staining) (Fig. 5 A and B a). Cell density within the hydrogel was evaluated by counting the number of CFDA-SE positive cells that we expressed as percentage, considering 100% of survival immediately after the implantation. Analyzing intravital microscopy at 3 days following positioning, the number of hMSCs in the HG RGD + ECM decreased to about 40% of the initial number, that became 15% at 9 days after the positioning (Fig. 5 B b).

3.5. Oriented delivery optimizes the fluidic release of factors from HG RGD + ECM in vivo

In order to demonstrate that a fluidic diffusion occurs from the hydrogel after implantation in the injury site *in vivo*, we evaluated the release profile of a fluorescent solution (Hoechst 33258) delivered by HG RGD + ECM. After 9 days from the HG RGD + ECM positioning in the lesion site, Hoechst 33258 fluorescence showed an evident intense signal mostly distributed in the epicenter of the injured site, whereas only few sections were stained outside the epicenter of the lesion (Fig. 6 a). This was confirmed by examining quantitatively the distribution of Hoechst 33258 staining in a portion of the spinal cord encompassing 12 mm around the epicenter of the injury (Fig. 6 a, d). In order to increase the fluidic diffusion from the hydrogel toward the injury site, we applied and tested an impermeable cling film that, sealing the hydrogel to the spinal cord, optimizes the fluidic diffusion toward the injury site (Fig. 6 b). Analyzing the Hoechst 33258 staining in spinal cord tissue after an oriented delivery (Fig. 6 b), we found a dramatic increase of fluorescent staining in both the epicenter and in regions outside the lesion, compared to unsealed hydrogel (Fig. 6 a). This was confirmed by evaluating quantitatively the distribution of the Hoechst 33258 staining in the spinal cord segments around the traumatized spinal cord (Fig. 6 c, d). These analyses demonstrated that a more oriented diffusion from the hydrogel, obtained by using a cling film, can potentially optimize a paracrine release of trophic factors toward the injured site, potentially increasing the therapeutic effect.

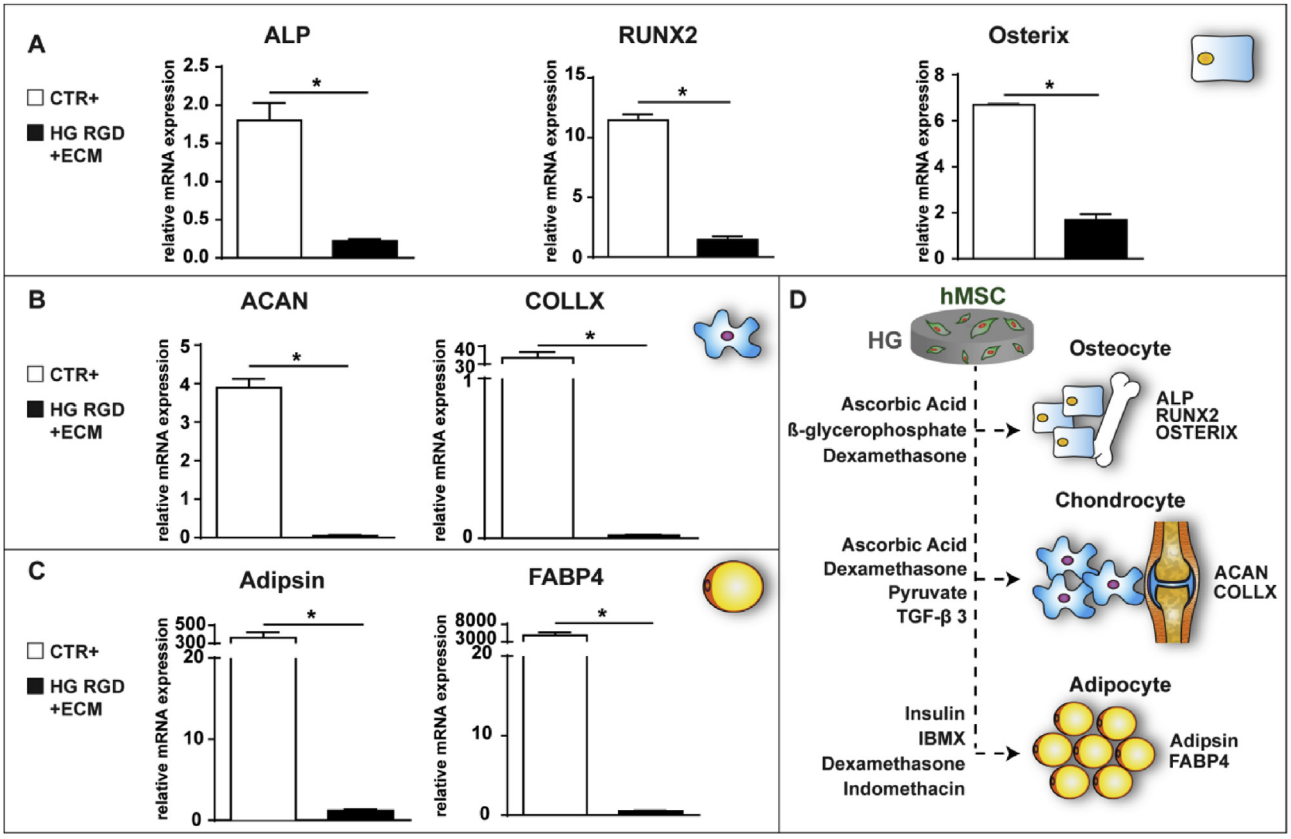

Fig. 4. mRNA analysis of hMSCs encapsulated within biomimetic scaffold. (A, B, C) Graphs representing the expression of specific genes related to three differentiation lineages: alkaline phosphatase (ALP), runt-related transcription factor 2 (RUNX2) and osterix for osteogenic differentiation; aggrecan (ACAN) and collagen type X (COLLX) for chondrogenic differentiation and adipsin and fatty acid binding-protein 4 (FABP4) for adipogenic differentiation. hMSCs encapsulated whithin HG RGD + ECM for 21 days are compared to the positive control represented by hMSCs loaded in HG RGD and treated with specific differentiating media for 21 days. Data are expressed as fold change compared to steady-state undifferentiated hMSCs (negative control). Statistical analysis: Mann Whitney test. Mean ± SEM is reported. (*) $p < 0.05$. $n = 3$ per group. (D) A representative cartoon of the three lineage commitments of hMSCs (osteocytes, chondrocytes and adipocytes) with respective principal pro-differentiating stimuli: ascorbic acid, β-glycerophosphate and dexamethasone to induce osteogenic differentiation; ascorbic acid, dexamethasone, pyruvate and TGF-β 3 to induce chondrogenic differentiation; insulin, 3-isobutyl-1-methylxanthine (IBMX), dexamethasone and indomethacin to induce adipogenic differentiation.

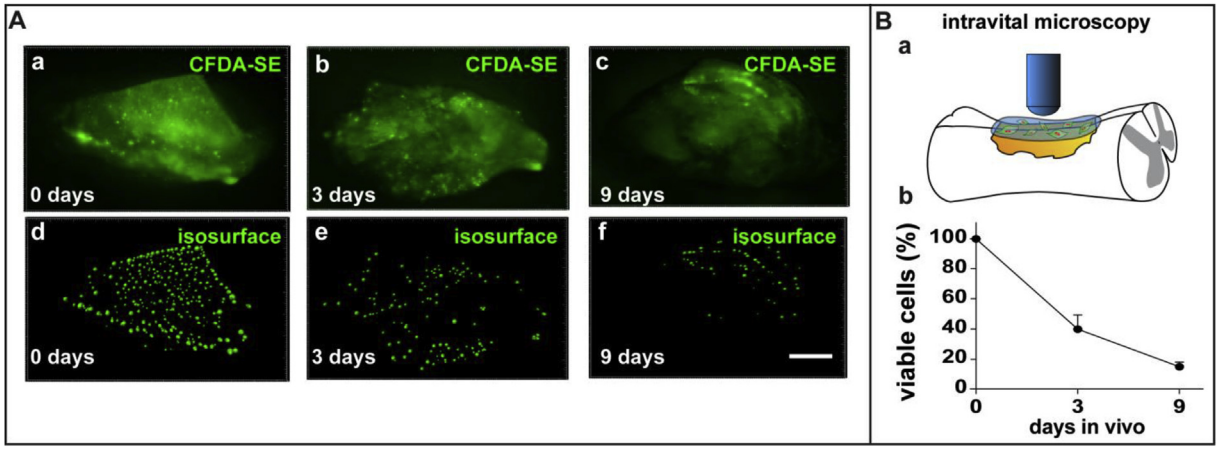

Fig. 5. hMSCs viability within HG RGD + ECM is revealed up to 9 days *in vivo*. (A) (a–c) Representative images of intravital acquisition of CFDA-SE positive hMSCs within HG RGD + ECM positioned in the injury site *in vivo*. Analysis has been performed immediately after the positioning (day 0, a and d) and at 3 (b and e) or 9 days (c and f) after the positioning. (d–f) The isosurfaces represent CFDA-SE positive cells considered for quantification of respective hydrogels. Scale bar represents 0.2 mm. (B) (a) Cartoon represents intravital acquisition of CFDA-SE positive hMSCs within HG RGD + ECM in the injury site. (b) Quantitative evaluation of viable hMSCs within HG RGD + ECM over time. Mean ± SEM is reported. $n = 8$.

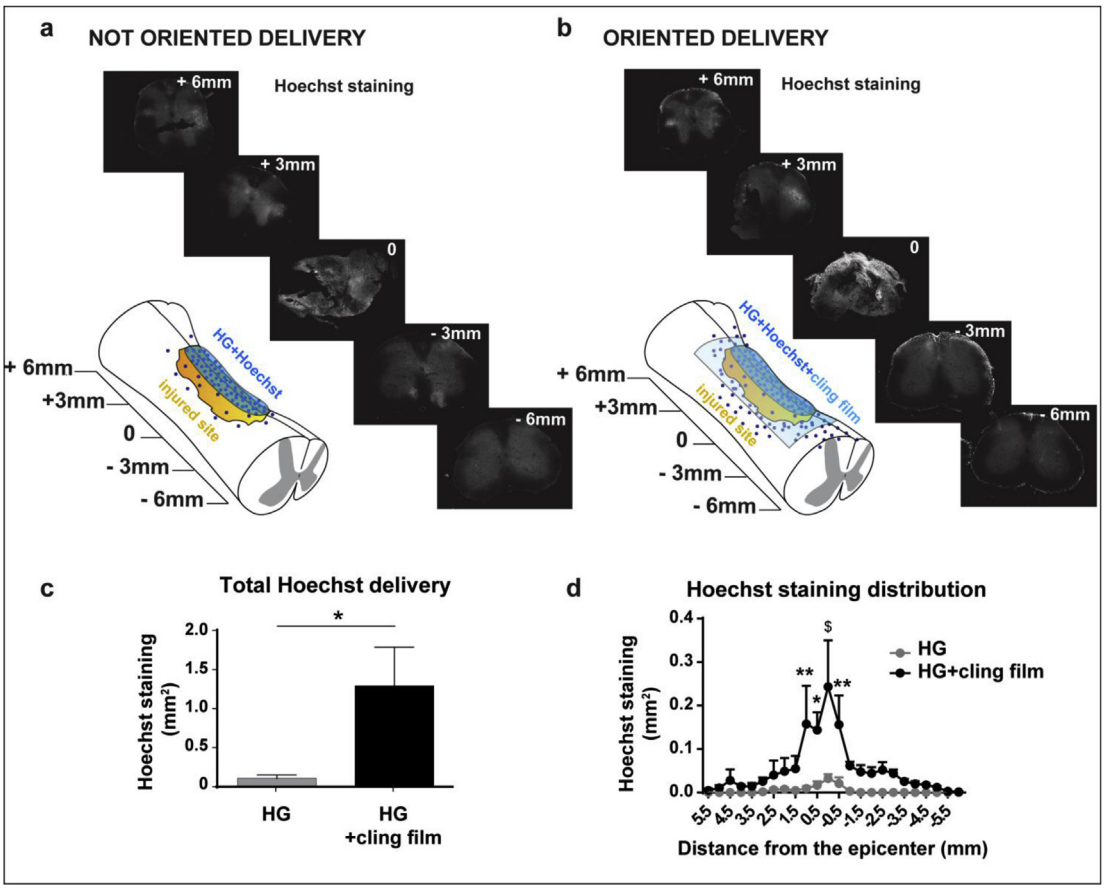

Fig. 6. Hoechst delivery from HG RGD + ECM *in vivo*. Release profile study of a fluorescent solution (Hoechst 33258) delivered by HG RGD + ECM in the injured site of the spinal cord. In a and b, representative images of Hoechst staining are shown in a portion of the spinal cord encompassing 12 mm around the epicenter of the injury. Cartoons show HG RGD + ECM positioning in both not oriented (a) and oriented delivery (b). Spinal cord after an oriented delivery shows a higher Hoechst staining as both total signal (c) and distribution around the epicenter (d) compared to unsealed hydrogel. Statistical analysis: Mann Whitney test for total Hoechst delivery (c), Two-way ANOVA followed by Bonferroni's post hoc test for Hoechst staining distribution (d). Mean ± SEM is reported. (*) $p < 0.05$, (**) $p < 0.01$, ($) $p < 0.0001$. n = 4 per group.

3.6. hMSCs loaded in HG RGD + ECM modulate inflammatory response in vivo

We assessed by FACS analysis whether hMSCs loaded in HG RGD + ECM sealed with cling film and implanted in the injured site were able to modulate, through a paracrine effect, resident microglia and recruited macrophages in the traumatized site, one therapeutic effect proposed in literature [60]. To distinguish between the two cell populations we performed, according to the literature [61–63], a double labeling with both CD11b and CD45 antibodies, identifying microglia by a $CD11b^{pos}/CD45^{low}$ signal and recruited macrophages by a $CD11b^{pos}/CD45^{high}$ signal (see Fig. S4 for gating). The amount of CD11b/CD45 positive labeled cells was evaluated in the injury epicenter. In response to SCI, resident microglia and recruited macrophages increased very early, even at 1 day post injury (DPI), reaching a peak of microglia activation and recruited macrophages migration in the damaged site at 7–9 DPI (data not shown). Mice treated with hMSCs loaded in HG RGD + ECM and analyzed at 9 DPI showed a significantly increased amount of recruited macrophages in the injured site (hMSCs, Fig. 7 A, b) compared to untreated mice (injury, Fig. 7 A, a), as demonstrated by dot plots (Fig. 7 A) and by quantitative analysis of microglia/macrophages ratio (Fig. 7 B). No changes were detected comparing FACS analysis of untreated injured mice (INJ) to injured mice treated with conditioned medium loaded within HG RGD + ECM (HG RGD + ECM + CM) or conditioned medium or hMSCs injected into the parenchyma (CM injected and hMSCs injected, respectively) (Fig. S5, A). These data demonstrated that only hMSCs loaded within HG RGD + ECM recruit more macrophages in the injured site via a paracrine effect. Furthermore, to investigate whether the proposed treatment was able to modulate M1 and/or M2 phenotypes in the injured site we performed a gene expression analysis to detect both M1 (IL-1β and TNFα) or M2 (Arg-I and YM1) phenotypes [60]. Analyzing both IL-1β and TNFα mRNA in the epicenter of the lesion in hMSCs loaded HG RGD + ECM + cling film treated mice at 9 DPI (Fig. 7C; a, b), only TNFα mRNA was detected significantly increased in treated injured mice (fold change of about 1.5) compared to the untreated injured mice (Fig. 7C; a). However, evaluating M2 mRNA markers in hMSCs loaded HG RGD + ECM + cling film treated mice, we demonstrated a significant increase of Arginase I M2-related transcript (Fig. 7C; d), but not of YM1 (Fig. 7C; c), compared to untreated injured mice. Noteworthy, Arginase I showed a mean fold change of about 10 compared to the untreated injured mice (Fig. 7C; d). No changes were detected by mRNA analysis comparing untreated injured mice (injury) to injured mice treated with either conditioned medium (CM injected) or hMSCs (hMSCs injected) injected in the parenchyma (Fig. S5, B). However, the analysis of IL-1β expression revealed higher levels of transcription in mice treated with conditioned medium loaded in HG RGD + ECM (HG RGD + ECM + CM, Fig. S4 B, b) compared to untreated mice (fold change of about 2.5), suggesting a partial effect of HG RGD + ECM scaffold in eliciting a polarization toward a pro-inflammatory M1 phenotype. Nevertheless, the treatment of mice with hMSCs loaded HG RGD + ECM

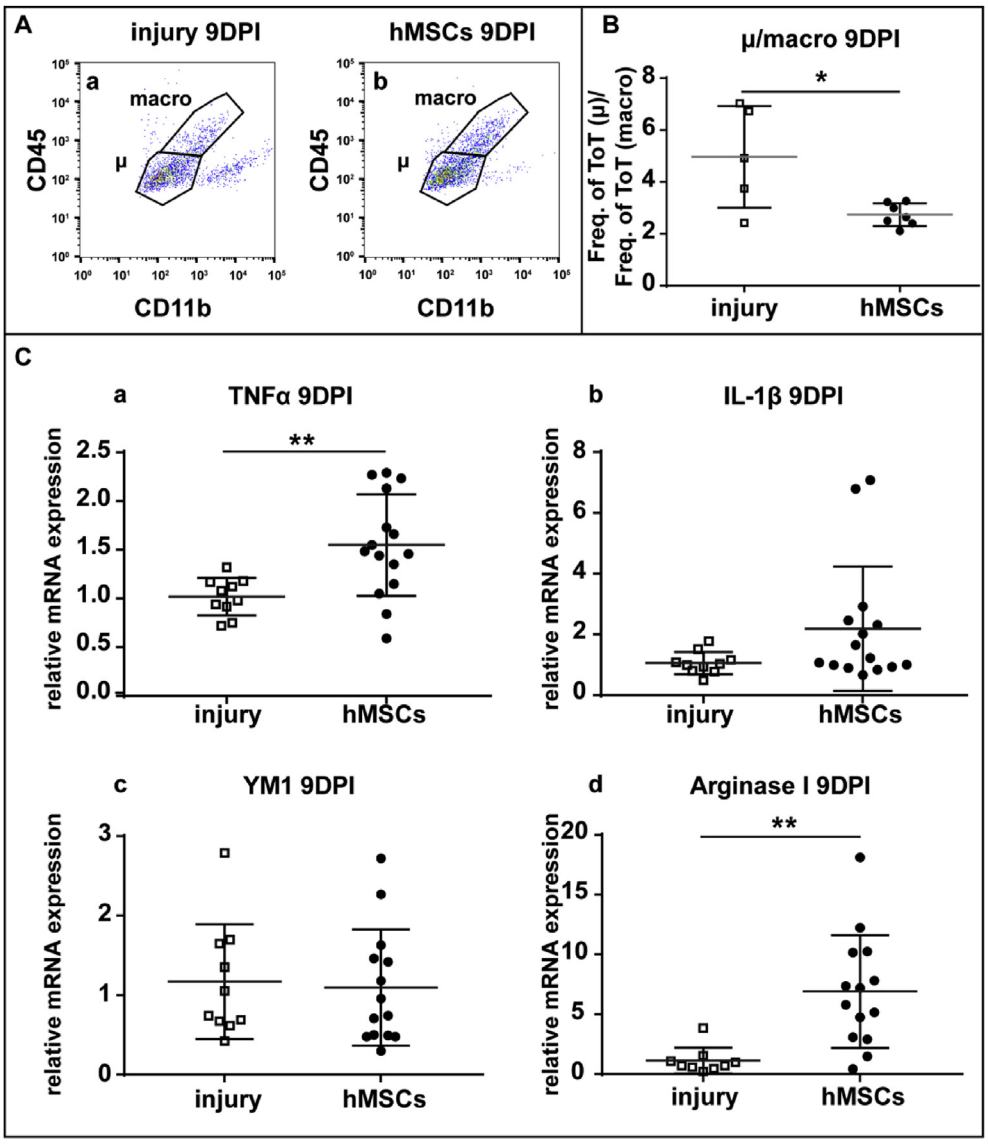

Fig. 7. hMSCs loaded in HG RGD + ECM modulate inflammatory response increasing M2 macrophages *in vivo*. (A) Representative FACS dot plots of microglial cells ($CD11b^{pos}/CD45^{low}$) and macrophages ($CD11b^{pos}/CD45^{high}$) present in SCI epicenter of untreated injured (injury, a) or hMSCs loaded within HG RGD + ECM treated injured mice (hMSCs, b) evaluated at 9 DPI (days post injury). An increased macrophages recruitment in hMSCs treated mice was found (b) compared to untreated mice (a). (B) Quantification of the ratio between microglia ($CD11b^{pos}/CD45^{low}$) and recruited macrophages ($CD11b^{pos}/CD45^{high}$) evaluated in untreated injured (injury) or hMSCs loaded within HG RGD + ECM treated injured mice (hMSCs) at 9 DPI. Graph shows a lower microglia/macrophages ratio in hMSCs group, demonstrating an increase of macrophages recruitment. Mean ± SEM is reported. Statistical analysis: Mann Whitney test. (*) $p < 0.05$. $n = 5–7$ mice per group. (C) Quantitative evaluation of mRNA expression of both M1 (TNFα, a and IL-1β, b) and M2 (YM1, c and Arginase I, d) markers of microglia/macrophages polarization in untreated injured (injury) or hMSCs loaded HG RGD + ECM treated injured mice (hMSCs) at 9 DPI. A significant increase of TNFα (about 1.5 folds) and Arginase I (about 10 folds) can be observed in mice treated with hMSCs compared to untreated injured mice, suggesting a skew toward an M2 pro-regenerative environment in hMSCs group. Mean ± SEM is reported. Statistical analysis: Mann Whitney test. (**) $p < 0.01$. $n = 10–14$ mice per group.

was able to revert the increased IL-1β expression, suggesting a further anti-inflammatory paracrine effect of hMSCs *in vivo* (Fig. 7C; b).

4. Discussion

Engineered scaffolds are considered a promising approach to create an optimal environment able to sustain a long lasting cell viability of stem cells in situ with the ability to help the tissue in terms of neuroprotection and neuroregeneration. These scaffolds offer the opportunity to deliver cells appropriately into the injured site optimizing the therapeutic effect of the treatment proposed. However, different limits have been revealed when these hMSCs have been encapsulated into biomaterials hampering their viability and a long lasting effect of the treatment. This was mostly due to the lack of an optimal combination of hMSCs, scaffold design and supporting environment that has limited the capability to support appropriate cell viability *in vitro* and *in vivo* [49]. It is well known that stem cell viability, phenotype and stemness are modulated by the interaction with the complex physicochemical composition of the natural niche mostly composed of ECM [43,55,64,65]. Therefore, the ECM could be considered a building block in sustaining hMSCs within biomaterial for maintaining a high viability and a high cellular density over time. In line with this idea, we here demonstrate and confirm that an optimal combination of an original hydrogel with a pre-constituted ECM deposited by hMSCs, together with an efficient stem cell loading (sponge-like effect), is an effective strategy to increase the viability and the cellular

density within an hydrogel for at least 21 days after seeding. In particular, in this study we establish that a lyophilized gel could be loaded through a soaked up effect preserving a higher cell viability compared to hMSCs loaded during the solution/gel transition. Reduced cell viability detected after a conventional loading procedure is likely due to the mechanical stress to which the cells are exposed [66], that is dramatically reduced loading hMSCs by a sponge-like effect. Furthermore, we demonstrate that RGD motif together with the pre-deposited 3D ECM has increased strongly the density of these cells within the hydrogel already at the first day after seeding. Furthermore, the 3D RGD ECM scaffold as here proposed significantly improves hMSCs maintenance showing a very high cell density up to 21 days *in vitro*. This time of survival is quite striking compared to other scaffolds proposed in literature where cells viability was observed only up to 7–14 days [48,67,68]. Furthermore, we demonstrate that a 3D ECM optimizes a healthy environment by converting hMSCs from a round shape to a spindle-like morphology, representing healthy cells indistinguishable from cells grown within a culture well. Differently, other groups reported a lower stem cells survival with a round shape morphology of hMSCs in the scaffold [48,67,68], suggesting that a spindle shape morphology is indicative of a cellular wellness that can contribute to the long term survival. We demonstrate also a preserved stemness of hMSCs during the time of analysis, confirming that a potential pleiotropic effect is maintained in this condition for a multitherapeutic approach in SCI. Altogether, these data confirm that a 3D ECM is a relevant support for the maintenance of hMSCs in this scaffold. So far, only few attempts have been made to mimic the physiological ECM directly within a biomaterial with the aim to optimize hMSCs viability [46–48,55,68–72]. Several studies used reconstituted monotypic ECM preparations in two dimensions to examine cell-matrix interactions and survival of the cells [55,71,72]. However, this represents a platform that does not constitute an optimal 3D native configuration, but only a 2D interactive structure [55,71,72]. It is well known that cell is affected by the physical environment in which it is grown. Indeed, in living tissue, cells reside in 3D microenvironments and establish many interactions with the surrounding matrix [73–75]. Moreover, cells in 3D culture exhibit different gene expression compared to cells in 2D [73] and provide different cell polarization, such as demonstrated in literature [73] and in our study. Indeed, a 3D framework provides more contact for cell adhesion, which is necessary for protein–protein ligation and cell-matrix signaling [73–75]. In addition, the architecture and conformation of the niche determines the mechanical properties of the ECM which in turn control cell adhesion, proliferation and differentiation [76]. For this reason, our 3D approach represents an optimal condition for cell culture where ECM is widely distributed in a 3D scaffold permitting a more appropriate environment for cell–cell interaction and polarization, and creates a more permissive environment similar to natural niche in which hMSCs can survive properly. Our approach is different also from previous studies whose attempts were to functionalize the scaffold with one single ECM peptide, as laminin, fibrin or RGD peptide [46–48,68,69], or to use a powdered ECM from porcine urinary bladder [70]. Indeed, ECM is composed of proteins, proteoglycans and factors able to establish a dynamic interaction with stem cells. Simultaneously, stem cells remodel actively the ECM in relation to their definite needs. Thus, only a few bioactive peptide sequences incorporated in synthetic hydrogels could represent only a partial support, but not an optimized environment to sustain hMSCs [46–48,68,69]. Therefore, to the best of our knowledge, this is the first study presenting a 3D natural ECM deposition able to increase adherence and viability of loaded hMSCs. *In vivo* experiments further demonstrate that a HG-RGD + ECM loaded with a fluorescent compound (Hoechst 33258) is efficiently implanted in the spinal cord and is able to release efficiently this molecule showing a sustainable delivery from the scaffold toward the injured site. To improve this delivery, we propose the use of an impermeable cling film that dramatically increases an oriented delivery toward the damaged site. Thus, we expect that, once implanted, hMSCs loaded HG-RGD + ECM + cling film will be able to release a higher concentration of factors in the injured spinal cord without any obstruction to their paracrine effect. This is confirmed by FACS and mRNA analyses demonstrating that a paracrine effect sustained by viable hMSCs loaded within HG RGD + ECM in just a few days is able to increase and/or convert efficaciously M2 macrophages (immunomodulation) in the injured site, promoting a pro-regenerative environment that represents a relevant outcome in treating SCI [26,50,77,78]. Noteworthy, injecting the same number of hMSCs directly in the parenchyma, a lack of efficacy is found in terms of macrophages recruitment or M1/M2 polarization. So far, the direct injection of hMSCs has been frequently proposed as preclinical SCI treatment, sometimes demonstrating a protective effect on histological or behavioral outcomes [13,79,80]. However, although a direct injection of stem cells may represent an attractive approach as clinical protocol, it shows deep concerns because very often stem cells leave the zone of injection, as they are not confined by any support. On the other hand, if injected stem cells remain in situ, they could be exposed to a hostile environment due to the tissue degeneration. Thus, a biomimetic scaffold, as proposed in this study, able to maintain MSCs viable, undifferentiated and confined within a 3D structure out of the degenerative environment is a forefront application. Moreover, the original scaffold material here proposed maximizes hMSCs paracrine protective effects, offering the possibility to reduce dramatically the cellular efficacious dose. Indeed, a consistent higher number of hMSCs is required when a direct injection is performed in situ to overcome mechanical forces that could damage stem cells passing from the needle [27] and concomitantly to preserve a sufficient number of them to counteract an inflamed and adverse environment present in the injured site [29,30].

In conclusion, we propose a new sustainable stem cell therapy by using HG RGD + ECM derived from the combination of different promising strategies such as: 1) a new loading procedure on a lyophilized scaffold (soaked up effect) that reduces mechanical stress and preserves hMSC viability when encapsulated into the hydrogel, 2) a RGD motif that increases the capacity to entrap hMSCs within the hydrogel after the seeding, 3) a 3D ECM deposition able to maintain over time healthy hMSCs with an high viability and density and 4) an oriented delivery of paracrine factors for treating efficaciously the injured site. We believe that the optimized scaffold as here proposed results to be a promising and innovative approach that may represent a breakthrough in using stem cells therapy supported by biomaterial with potential beneficial impact on SCI.

Acknowledgments

Authors' research is supported by Ministry of Health (GR-2010-2312573).

Appendix A. Supplementary data

Supplementary data related to this article can be found at http://dx.doi.org/10.1016/j.biomaterials.2015.10.024.

References

[1] G. Onose, A. Anghelescu, D.F. Muresanu, L. Padure, M.A. Haras, C.O. Chendreanu, et al., A review of published reports on neuroprotection in

spinal cord injury, Spinal Cord 47 (2009) 716–726.
[2] G.W. Hawryluk, J. Rowland, B.K. Kwon, M.G. Fehlings, Protection and repair of the injured spinal cord: a review of completed, ongoing, and planned clinical trials for acute spinal cord injury, Neurosurg. Focus 25 (2008) E14.
[3] B.K. Kwon, E. Okon, J. Hillyer, C. Mann, D. Baptiste, L.C. Weaver, et al., A systematic review of non-invasive pharmacologic neuroprotective treatments for acute spinal cord injury, J. Neurotrauma 28 (2011) 1545–1588.
[4] B.K. Kwon, E.B. Okon, W. Plunet, D. Baptiste, K. Fouad, J. Hillyer, et al., A systematic review of directly applied biologic therapies for acute spinal cord injury, J. Neurotrauma 28 (2011) 1589–1610.
[5] N.A. Silva, N. Sousa, R.L. Reis, A.J. Salgado, From basics to clinical: a comprehensive review on spinal cord injury, Prog. Neurobiol. 114 (2014) 25–57.
[6] S. Lee, E. Choi, M.J. Cha, K.C. Hwang, Cell adhesion and long-term survival of transplanted mesenchymal stem cells: a prerequisite for cell therapy, Oxid. Med. Cell. Longev. 2015 (2015) 632902.
[7] S. Thuret, L.D. Moon, F.H. Gage, Therapeutic interventions after spinal cord injury, Nat. Rev. Neurosci. 7 (2006) 628–643.
[8] R. Adami, G. Scesa, D. Bottai, Stem cell transplantation in neurological diseases: improving effectiveness in animal models, Front. Cell Dev. Biol. 2 (2014) 17.
[9] M.F. Azari, L. Mathias, E. Ozturk, D.S. Cram, R.L. Boyd, S. Petratos, Mesenchymal stem cells for treatment of CNS injury, Curr. Neuropharmacol. 8 (2010) 316–323.
[10] S. Forostyak, P. Jendelova, E. Sykova, The role of mesenchymal stromal cells in spinal cord injury, regenerative medicine and possible clinical applications, Biochimie 95 (2013) 2257–2270.
[11] R. Vawda, M.G. Fehlings, Mesenchymal cells in the treatment of spinal cord injury: current & future perspectives, Curr. Stem Cell Res. Ther. 8 (2013) 25–38.
[12] X. Liang, Y. Ding, Y. Zhang, H.F. Tse, Q. Lian, Paracrine mechanisms of mesenchymal stem cell-based therapy: current status and perspectives, Cell Transplant. 23 (2014) 1045–1059.
[13] V.R. Dasari, D.G. Spomar, C.S. Gondi, C.A. Sloffer, K.L. Saving, M. Gujrati, et al., Axonal remyelination by cord blood stem cells after spinal cord injury, J. Neurotrauma 24 (2007) 391–410.
[14] S. Wislet-Gendebien, F. Wautier, P. Leprince, B. Rogister, Astrocytic and neuronal fate of mesenchymal stem cells expressing nestin, Brain Res. Bull. 68 (2005) 95–102.
[15] A.I. Caplan, D. Correa, The MSC: an injury drugstore, Cell Stem Cell 9 (2011) 11–15.
[16] S.A. Hardy, D.J. Maltman, S.A. Przyborski, Mesenchymal stem cells as mediators of neural differentiation, Curr. Stem Cell Res. Ther. 3 (2008) 43–52.
[17] J.R. Lavoie, M. Rosu-Myles, Uncovering the secretes of mesenchymal stem cells, Biochimie 95 (2013) 2212–2221.
[18] G. Paul, S.V. Anisimov, The secretome of mesenchymal stem cells: potential implications for neuroregeneration, Biochimie 95 (2013) 2246–2256.
[19] J.D. Glenn, K.A. Whartenby, Mesenchymal stem cells: emerging mechanisms of immunomodulation and therapy, World J. Stem Cells 6 (2014) 526–539.
[20] K. Le Blanc, D. Mougiakakos, Multipotent mesenchymal stromal cells and the innate immune system, Nat. Rev. Immunol. 12 (2012) 383–396.
[21] A. Uccelli, V. Pistoia, L. Moretta, Mesenchymal stem cells: a new strategy for immunosuppression? Trends Immunol. 28 (2007) 219–226.
[22] M.T. Harting, F. Jimenez, H. Xue, U.M. Fischer, J. Baumgartner, P.K. Dash, et al., Intravenous mesenchymal stem cell therapy for traumatic brain injury, J. Neurosurg. 110 (2009) 1189–1197.
[23] U.M. Fischer, M.T. Harting, F. Jimenez, W.O. Monzon-Posadas, H. Xue, S.I. Savitz, et al., Pulmonary passage is a major obstacle for intravenous stem cell delivery: the pulmonary first-pass effect, Stem Cells Dev. 18 (2009) 683–692.
[24] M.B. Potts, M.T. Silvestrini, D.A. Lim, Devices for cell transplantation into the central nervous system: design considerations and emerging technologies, Surg. Neurol. Int. 4 (2013) S22–S30.
[25] J.W. Jung, M. Kwon, J.C. Choi, J.W. Shin, I.W. Park, B.W. Choi, et al., Familial occurrence of pulmonary embolism after intravenous, adipose tissue-derived stem cell therapy, Yonsei Med. J. 54 (2013) 1293–1296.
[26] F. Rossi, G. Perale, S. Papa, G. Forloni, P. Veglianese, Current options for drug delivery to the spinal cord, Expert Opin. Drug Deliv. 10 (2013) 385–396.
[27] B.A. Aguado, W. Mulyasasmita, J. Su, K.J. Lampe, S.C. Heilshorn, Improving viability of stem cells during syringe needle flow through the design of hydrogel cell carriers, Tissue Eng. Part A 18 (2012) 806–815.
[28] F. Cao, A.H. Sadrzadeh Rafie, O.J. Abilez, H. Wang, J.T. Blundo, B. Pruitt, et al., In vivo imaging and evaluation of different biomatrices for improvement of stem cell survival, J. Tissue Eng. Regen. Med. 1 (2007) 465–468.
[29] T.E. Robey, M.K. Saiget, H. Reinecke, C.E. Murry, Systems approaches to preventing transplanted cell death in cardiac repair, J. Mol. Cell. Cardiol. 45 (2008) 567–581.
[30] M.J. Cooke, aK. Vulicb, M.S. Shoichet, Design of biomaterials to enhance stem cell survival when transplanted into the damaged central nervous system, Soft Matter 6 (2010) 4988–4998.
[31] B. Shrestha, K. Coykendall, Y. Li, A. Moon, P. Priyadarshani, L. Yao, Repair of injured spinal cord using biomaterial scaffolds and stem cells, Stem Cell Res. Ther. 5 (2014) 91.
[32] J. Thiele, Y. Ma, S.M. Bruekers, S. Ma, W.T. Huck, 25th anniversary article: designer hydrogels for cell cultures: a materials selection guide, Adv. Mater. 26 (2014) 125–147.
[33] G. Perale, F. Rossi, E. Sundstrom, S. Bacchiega, M. Masi, G. Forloni, et al., Hydrogels in spinal cord injury repair strategies, ACS Chem. Neurosci. 2 (2011) 336–345.
[34] D. Albani, A. Gloria, C. Giordano, S. Rodilossi, T. Russo, U. D'Amora, et al., Hydrogel-based nanocomposites and mesenchymal stem cells: a promising synergistic strategy for neurodegenerative disorders therapy, Sci. World J. 2013 (2013) 270260.
[35] A. Moshaverinia, C. Chen, X. Xu, S. Ansari, H.H. Zadeh, S.R. Schricker, et al., Regulation of the stem cell-host immune system interplay using hydrogel coencapsulation system with an anti-inflammatory drug, Adv. Funct. Mater. 25 (2015) 2296–2307.
[36] O. Jeon, E. Alsberg, Regulation of stem cell fate in a three-dimensional micropatterned dual-crosslinked hydrogel system, Adv. Funct. Mater. 23 (2013) 4765–4775.
[37] S. Ribeiro-Samy, N.A. Silva, V.M. Correlo, J.S. Fraga, L. Pinto, A. Teixeira-Castro, et al., Development and characterization of a PHB-HV-based 3D scaffold for a tissue engineering and cell-therapy combinatorial approach for spinal cord injury regeneration, Macromol. Biosci. 13 (2013) 1576–1592.
[38] J. Wang, J. Zhang, X. Zhang, H. Zhou, A protein-based hydrogel for in vitro expansion of mesenchymal stem cells, PLoS One 8 (2013) e75727.
[39] X. Zeng, Y.S. Zeng, Y.H. Ma, L.Y. Lu, B.L. Du, W. Zhang, et al., Bone marrow mesenchymal stem cells in a three-dimensional gelatin sponge scaffold attenuate inflammation, promote angiogenesis, and reduce cavity formation in experimental spinal cord injury, Cell Transplant. 20 (2011) 1881–1899.
[40] A.J. Mothe, R.Y. Tam, T. Zahir, C.H. Tator, M.S. Shoichet, Repair of the injured spinal cord by transplantation of neural stem cells in a hyaluronan-based hydrogel, Biomaterials 34 (2013) 3775–3783.
[41] I. Zvibel, F. Smets, H. Soriano, Anoikis: roadblock to cell transplantation? Cell Transplant. 11 (2002) 621–630.
[42] X.D. Chen, Extracellular matrix provides an optimal niche for the maintenance and propagation of mesenchymal stem cells, Birth Defects Res. Part C 90 (2010) 45–54.
[43] F. Guilak, D.M. Cohen, B.T. Estes, J.M. Gimble, W. Liedtke, C.S. Chen, Control of stem cell fate by physical interactions with the extracellular matrix, Cell Stem Cell 5 (2009) 17–26.
[44] L. Coulombel, M.H. Vuillet, C. Leroy, G. Tchernia, Lineage- and stage-specific adhesion of human hematopoietic progenitor cells to extracellular matrices from marrow fibroblasts, Blood 71 (1988) 329–334.
[45] T. Matsubara, S. Tsutsumi, H. Pan, H. Hiraoka, R. Oda, M. Nishimura, et al., A new technique to expand human mesenchymal stem cells using basement membrane extracellular matrix, Biochem. Biophys. Res. Commun. 313 (2004) 503–508.
[46] A. Hejcl, J. Sedy, M. Kapcalova, D.A. Toro, T. Amemori, P. Lesny, et al., HPMA-RGD hydrogels seeded with mesenchymal stem cells improve functional outcome in chronic spinal cord injury, Stem Cells Dev. 19 (2010) 1535–1546.
[47] J. Park, E. Lim, S. Back, H. Na, Y. Park, K. Sun, Nerve regeneration following spinal cord injury using matrix metalloproteinase-sensitive, hyaluronic acid-based biomimetic hydrogel scaffold containing brain-derived neurotrophic factor, J. Biomed. Mater. Res. A 93 (2010) 1091–1099.
[48] S.B. Anderson, C.C. Lin, D.V. Kuntzler, K.S. Anseth, The performance of human mesenchymal stem cells encapsulated in cell-degradable polymer-peptide hydrogels, Biomaterials 32 (2011) 3564–3574.
[49] F.Z. Volpato, T. Führmann, C. Migliaresi, D.W. Hutmacher, P.D. Dalton, Using extracellular matrix for regenerative medicine in the spinal cord, Biomaterials 34 (2013) 4945–4955.
[50] G. Perale, F. Rossi, M. Santoro, M. Peviani, S. Papa, D. Llupi, et al., Multiple drug delivery hydrogel system for spinal cord injury repair strategies, J. Control. Release 159 (2012) 271–280.
[51] A. Sacchetti, E. Mauri, M. Sani, M. Masi, F. Rossi, Microwave-assisted synthesis and click chemistry as simple and efficient strategy for RGD functionalized hydrogels, Tetrahedron Lett. 55 (2014) 6817–6820.
[52] M. Barilani, C. Lavazza, M. Vigano, T. Montemurro, V. Boldrin, V. Parazzi, et al., Dissection of the cord blood stromal component reveals predictive parameters for culture outcome, Stem Cells Dev. 24 (2015) 104–114.
[53] L.C. Junquiera, L.C. Junqueira, R.R. Brentani, A simple and sensitive method for the quantitative estimation of collagen, Anal. Biochem. 94 (1979) 96–99.
[54] A. Lopez-De Leon, M. Rojkind, A simple micromethod for collagen and total protein determination in formalin-fixed paraffin-embedded sections, J. Histochem. Cytochem. 33 (1985) 737–743.
[55] M.C. Prewitz, F.P. Seib, M. von Bonin, J. Friedrichs, A. Stissel, C. Niehage, et al., Tightly anchored tissue-mimetic matrices as instructive stem cell microenvironments, Nat. Methods 10 (2013) 788–794.
[56] T.M. Liu, E.H. Lee, Transcriptional regulatory cascades in Runx2-dependent bone development, Tissue Eng. Part B Rev. 19 (2013) 254–263.
[57] F. Barry, R.E. Boynton, B. Liu, J.M. Murphy, Chondrogenic differentiation of mesenchymal stem cells from bone marrow: differentiation-dependent gene expression of matrix components, Exp. Cell Res. 268 (2001) 189–200.
[58] M. Kamata, Y. Okitsu, T. Fujiwara, M. Kanehira, S. Nakajima, T. Takahashi, et al., GATA2 regulates differentiation of bone marrow-derived mesenchymal stem cells, Haematologica 99 (2014) 1686–1696.
[59] E. Ragni, M. Vigano, P. Rebulla, R. Giordano, L. Lazzari, What is beyond a qRT-PCR study on mesenchymal stem cell differentiation properties: how to choose the most reliable housekeeping genes, J. Cell. Mol. Med. 17 (2013) 168–180.
[60] E.R. Zanier, F. Pischiutta, L. Riganti, F. Marchesi, E. Turola, S. Fumagalli, et al.,

Bone marrow mesenchymal stromal cells drive protective M2 microglia polarization after brain trauma, Neurotherapeutics 11 (2014) 679–695.
[61] A.L. Ford, A.L. Goodsall, W.F. Hickey, J.D. Sedgwick, Normal adult ramified microglia separated from other central nervous system macrophages by flow cytometric sorting. Phenotypic differences defined and direct ex vivo antigen presentation to myelin basic protein-reactive CD4+ T cells compared, J. Immunol. 154 (1995) 4309–4321.
[62] A. Capotondo, R. Milazzo, L.S. Politi, A. Quattrini, A. Palini, T. Plati, et al., Brain conditioning is instrumental for successful microglia reconstitution following hematopoietic stem cell transplantation, Proc. Natl. Acad. Sci. U. S. A. 109 (2012) 15018–15023.
[63] D.P. Stirling, V.W. Yong, Dynamics of the inflammatory response after murine spinal cord injury revealed by flow cytometry, J. Neurosci. Res. 86 (2008) 1944–1958.
[64] G. Pennesi, S. Scaglione, P. Giannoni, R. Quarto, Regulatory influence of scaffolds on cell behavior: how cells decode biomaterials, Curr. Pharm. Biotechnol. 12 (2011) 151–159.
[65] S.F. Badylak, D.O. Freytes, T.W. Gilbert, Extracellular matrix as a biological scaffold material: structure and function, Acta Biomater. 5 (2009) 1–13.
[66] D.M. Cohen, C.S. Chen, Mechanical control of stem cell differentiation, StemBook, Cambridge (MA), 2008.
[67] H.K. Cheung, T.T. Han, D.M. Marecak, J.F. Watkins, B.G. Amsden, L.E. Flynn, Composite hydrogel scaffolds incorporating decellularized adipose tissue for soft tissue engineering with adipose-derived stem cells, Biomaterials 35 (2014) 1914–1923.
[68] F.R. Maia, K.B. Fonseca, G. Rodrigues, P.L. Granja, C.C. Barrias, Matrix-driven formation of mesenchymal stem cell-extracellular matrix microtissues on soft alginate hydrogels, Acta Biomater. 10 (2014) 3197–3208.
[69] K. Marycz, D. Szarek, J. Grzesiak, K. Wrzeszcz, Influence of modified alginate hydrogels on mesenchymal stem cells and olfactory bulb-derived glial cells cultures, Bio-Med Mater. Eng. 24 (2014) 1625–1637.
[70] L. Penolazzi, G. Lisignoli, E. Lambertini, E. Torreggiani, C. Manferdini, A. Lolli, et al., Transcription factor decoy against NFATc1 in human primary osteoblasts, Int. J. Mol. Med. 28 (2011) 199–206.
[71] M.J. Cooke, T. Zahir, S.R. Phillips, D.S. Shah, D. Athey, J.H. Lakey, et al., Neural differentiation regulated by biomimetic surfaces presenting motifs of extracellular matrix proteins, J. Biomed. Mater. Res. A 93 (2010) 824–832.
[72] X.D. Chen, V. Dusevich, J.Q. Feng, S.C. Manolagas, R.L. Jilka, Extracellular matrix made by bone marrow cells facilitates expansion of marrow-derived mesenchymal progenitor cells and prevents their differentiation into osteoblasts, J. Bone Min. Res. 22 (2007) 1943–1956.
[73] F. Pampaloni, E.G. Reynaud, E.H. Stelzer, The third dimension bridges the gap between cell culture and live tissue, Nat. Rev. Mol. Cell Biol. 8 (2007) 839–845.
[74] G.D. Prestwich, Simplifying the extracellular matrix for 3-D cell culture and tissue engineering: a pragmatic approach, J. Cell. Biochem. 101 (2007) 1370–1383.
[75] J. Lee, M.J. Cuddihy, N.A. Kotov, Three-dimensional cell culture matrices: state of the art, Tissue Eng. Part B Rev. 14 (2008) 61–86.
[76] L.G. Griffith, M.A. Swartz, Capturing complex 3D tissue physiology in vitro, Nat. Rev. Mol. Cell Biol. 7 (2006) 211–224.
[77] I. Caron, S. Papa, F. Rossi, G. Forloni, P. Veglianese, Nanovector-mediated drug delivery for spinal cord injury treatment, Wiley Interdiscip. Rev. Nanomed. Nanobiotechnol. 6 (2014) 506–515.
[78] S. Papa, F. Rossi, R. Ferrari, A. Mariani, M. De Paola, I. Caron, et al., Selective nanovector mediated treatment of activated proinflammatory microglia/macrophages in spinal cord injury, ACS Nano 7 (2013) 9881–9895.
[79] C. Mannoji, M. Koda, K. Kamiya, M. Dezawa, M. Hashimoto, T. Furuya, et al., Transplantation of human bone marrow stromal cell-derived neuroregenerative cells promotes functional recovery after spinal cord injury in mice, Acta Neurobiol. Exp. 74 (2014) 479–488.
[80] H. Nakajima, K. Uchida, A.R. Guerrero, S. Watanabe, D. Sugita, N. Takeura, et al., Transplantation of mesenchymal stem cells promotes an alternative pathway of macrophage activation and functional recovery after spinal cord injury, J. Neurotrauma 29 (2012) 1614–1625.